1986

Characteristics of Compressor for a Room Air Conditioner Using a Non-Azeotropic Mixture of Refrigerants

H. Matsunaga

H. Hirano

K. Uchiyama

K. Nakatani

CHARACTERISTICS OF COMPRESSOR FOR A ROOM AIR CONDITIONER USING A NON-AZEOTROPIC MIXTURE OF REFRIGERANTS

Hiroshi Matsunaga[1], Hideo Hirano[2], Kuniyasu Uchiyama[3] and Kazuo Nakatani[4]
[1]Engineer, Compressor Division, [2]Chief Engineer, Air-Conditioner Division, [3]Chief Engineer, Air-Conditioner Division, [4]Engineer, Corporate Engineering Division, Matsushita Electric Industrial Co., Ltd. (PANASONIC), Noji-Cho, Kusatsu 525, JAPAN

ABSTRACT

As is well known, the most popular refrigerant used in air conditioning machines today is freon 22, but non-azeotropic mixtures have recently been receiving much attention. The non-azeotropic mixtures have various excellent characteristics that the single component refrigerants do not possess. However, very limited information has been available on the commercial exploitation of an air conditioning system using such a non-azeotropic mixture.

We have succeeded in developing a split-type heat pump room air conditioner employing a non-azeotropic mixture, which can be used effectively, especially in cold districts. The use of a refrigerant mixture calls for the development of a new compressor design. The compressor developed for the non-azeotropic mixture is an inverter-driven rolling piston rotary compressor which can be operated at 30 Hz to 120 Hz. This report presents the performance of the room air conditioner using a new non-azeotropic refrigerant mixture and the design and characteristics of the compressor.

INTRODUCTION

The greatest disadvantage of an air-source heat pump is that its capacity and EER decrease with a decreasing outdoor temperature. Of course, the lower the outdoor temperature, the larger is the heating capacity required. This has imposed limitations on the use of air-source heat pumps in cold districts. To relieve the limitations even just a little, it has been proposed to provide the room air conditioner with a built-in heater to make up for the deficiency in its heating capacity, or to employ a high-power compressor to provide spare heating capacity. However, both methods detract from the high EER characteristic which is a major advantage of the heat pump.

Recently, in Japan, an inverter-driven compressor has been mainly used in room air conditioners. In the inverter type air conditioner, one may drive the compressor at a high frequency when a large heating capacity is required so as to leave spare capacity and lower the frequency when the demand for capacity is small. This measure resulted in a marked improvement in heating capacity under low outdoor temperature conditions. However, none of the systems so far proposed have been successfully developed into actual products having a heating capacity commensurate with use in cold districts and a practically meaningful level of EER.

In order to improve the energy efficiency at low outdoor temperature, we saw a limit to the current monocomponent refrigerant R22 and researched for a new refrigerant having improved low temperature characteristics.

As a result, we selected a non-azeotropic binary refrigerant consisting of 30% of R13B1, which is lower-boiling than R22, and 70% of the R22. By using this new binary refrigerant in combination with the inverter drive, we could improve the characteristics at low outdoor temperature and succeeded in the development of a room air conditioner which can be used effectively in cold districts. In this report, the performance of the newly developed room air conditioner and the major characteristics of the inverter-driven compressor are presented.

OUTLINE OF THE AIR CONDITIONER

Fig. 1 is an exterior view showing a new air conditioner. Of the split-type, the air conditioner consists of an outdoor unit comprising an inverter drive and a compressor and an indoor unit which is equipped with a remote controller. Each of the units has a built-in microcomputer for automatic control of the compressor, the fan, etc.

Table 1 shows the basic specifications of the new air conditioner.

Fig. 2 shows a basic refrigeration cycle. Defrosting is performed by switching a 4-way reversing valve.

Table 1

Capacity	Cooling	2240 kcal/h
	Heating	3300 kcal/h
	Electric sourse	1 ϕ 100 V 50/60 Hz
Electric power	Cooling	1025 W
	Heating	1320 W
Compressor		Rolling piston, rotary
refrigerant		R22 + R13B1, 1000 g

COMPARISON WITH THE CONVENTIONAL PRODUCT

Table 2 shows the characteristics of an air conditioner utilizing a high capacity compressor with a heater compared with those of the new binary refrigerant-inverter air conditioner.

Table 2

		Heating capacity			Cooling capacity	Note
		Rated condition	0°C	-7°C	Rated condition	(electric heater)
CS-220GR	Capacity (kcal/h)	3,300	3,400	3,100	2,240	—
	Electric power (W)	1,320	—	—	1,025	
CS-2220AK5F	Capacity (kcal/h)	4,300	3,660	3,000	2,240	850 W
	Electric power (W)	2,100	—	—	1,080	

It is apparent that the new air conditioner has a higher capacity at low outdoor temperature and an improved heating EER.

Compared with the conventional product, an improvement in efficiency of about 20% has been accomplished.

The above improvements have not been realized by the mere adoption of the new binary refrigerant but have been made possible by the use of inverter drive, improvements in the heat exchanger, and optimization of the refrigeration cycle for the new refrigerant. It is very difficult to isolate these elements, however.

THE BINARY REFRIGERANT

Physical properties

The fundamental properties of R22 and R13B1, which constitute the binary refrigerant, are given in Table 3.

Table 3

	Unit	R13B1	R22
Chemical formula		$CBrF_3$	$CHClF_2$
Boiling point	(1 atm) °C	-57.823	-40.75
Molecular weight		148.91	86.47
Freezing point	°C	-168	-160
Critical temperature	°C	66.9	96.0
Critical pressure	atm	39.1	49.12
Critical volume	cc/mol	200	165
Critical density	g/cc	0.745	0.525
Evaporating latent heat	(Boiling point) kcal/kg	28.38	55.81
Flammability		None	None
Toxicity		6	5A

The physical constants of a varying mixture of these component refrigerants were computed according to a multi-component system physical property estimation program developed at Matsushita. (In this program, Soave's equation for the RK system and the mixture rule including an interaction parameters are applied to the vapor-liquid coexisting phase)(1).

The results of the above estimation are shown in Figs. 3 and 4. Fig. 3 shows the cooling capacity per unit volume of refrigerant and the theoretical cooling COP for a varying mixture of R13B1 and R22 under the basic temperature conditions simulating a cooling operation. Fig. 4 shows the heating capacity per unit volume of refrigerant and the theoretical heating COP under the basic temperature conditions simulating a low-temperature heating operation. Both conditions are based on the vapor phase.

From these diagrams, it can be seen: The larger the proportion of R13B1 which is lower-boiling, the higher is the capacity. The degree of increase in capacity is remarkable under temperature conditions simulating a low-temperature heating operation where the evaporation temperature is low COP tends to decrease with an increasing proportion of the lower-boiling R13B1. This tendency is more remarkable under temperature conditions close to a cooling operation.

Fig. 5 is a pressure-enthalpy diagram for a 30/70 (%) mixture of R13B1 and R22 as computed according to the above-mentioned estimation program. The isothermal line in the vapor-liquid coexisting phase, which is characteristic of a non-azeotropic mixture, is inclined.

Thus, when R13B1 and R22 are used in admixture, both the capacity and EER are increased at low outdoor temperature where the evaporation temperature is low. However, the decrease of EER is large under conditions where the evaporation temperature is high.

The decrease of EER is greater with an increasing proportion of R13B1, and when R13B1 was used alone, a significant decrease of EER occurred in the cooling operation. Taking these phenomena into account, the optimum R13B1/R22 ratio was considered to be 30/70 (%). This binary refrigerant will be referred to as refrigerant mixture M1.

High Heating Capacity in Cold Districts

In order to evaluate the effects induced by using refrigerant mixture M1, the same air conditioner was operated on the refrigerant mixture M1 as well as on R22 and the respective performances were compared. An inverter-driven variable-speed compressor was used. The same heat exchangers and fan were used for both trials. The throttling amount and refrigerant charge were optimized for the respective refrigerants.

Fig. 6 shows the characteristics for R22 and R13B1/R22 under varying outdoor temperatures. It is apparent that refrigerant mixture M1 contributes to a capacity increase of 10 to 12% when the same compressor is driven at the same frequency and that the degree of increase is greater when the outdoor temperature is lower.

It is thus clear, that assuming a limit (e.g. 98 Hz) to the frequency of the inverter-driven compressor using R13B1 enables one to achieve an increased heating capacity especially under low outdoor temperature conditions.

A further important parameter is EER. Figs. 7 and 8 show comparisons between R22 and refrigerant mixture M1 with capacity plotted on the horizontal axis and the air conditioner heating capacity-to-compressor input ratio, as an indicator of EER, on the vertical axis, assuming the same capacity as an air conditioner.

Figs. 7 and 8 correspond to the outdoor temperatures of 7°C and -7°C, respectively.

At the outdoor temperature of 7°C, the EER is slightly higher with the single-component refrigerant R22. However, when the outdoor temperature is -7°C, the refrigerant mixture M1 ensures an improved EER.

Outline of Construction

Fig. 9a shows a cross section of a single-cylinder refrigerant compressor of the rolling-piston rotary type.

The rolling piston compressor used in the new room air conditioner is shown in Fig. 9a.

The electric motor is enclosed in the upper section within a sealed housing, and the compressor components are enclosed in the lower section. The compressor components are partially immersed in 410 cc of lubicating oil. The diameter of the housing is 132 mm in diameter and 230 mm in length, and the mass of the whole compressor is 14.5 kg. Fig. 9b is a top view of the A-A' cutting plane shown in Fig. 9a.

The cylinder volume is 12.86 cc. The electric motor is a 3 phase induction motor which can be driven by an inverter in the frequency range of 30 to 120 Hz. The diameter of the accumulator is 75 mm.

Major Performance Characteristics

Table 5 shows the performance characteristics of the compressor under rated temperature conditions, for each of the refrigerants.

Table 4

		R22	R13B1
	Temp. (°C)	Pressure (kgf/cm^2)	Pressure (gas region)
Evaporating temp.	7	6.33	7.26
Condensing temp.	55	22.18	25.05
Suction temp.	18	—	—

As the pressure-enthalpy diagram of the refrigerant mixture M1 is different from that of R22, the evaporation temperature and condensation temperature based on the vapor phase are taken as the rated temperature conditions.

Figs. 10 and 11 show the performance curves of varying the frequency under the above rated temperatrue conditions.

Fig. 10 shows the volume efficiency, discharge temperature and r.p.m. Fig. 11 shows the EER, the energy input and the heating capacity curves. Judging from the above curves, for both R22 and the refrigerant mixture M1, the volume efficiency increases with frequency and though it is generally higher for R22, the values become equal in the vicinity 120 Hz. Except at 30 Hz, the discharge temperature does not change much. The high discharge temperature value for the refrigerant mixture M1 at 30 Hz is due to the large input by the inverter drive.

- The flow rate is greater for the refrigerant mixture M1 throughout the frequency range at 120 Hz, it is 25% greater, assuming that the volume efficiency is the same.

- As both heating the capacity and the energy input are larger for the refrigerant mixture M1 and the difference of input is greater than that of heating capacity, the EER is lower for the refrigerant mixture under previously prescribed temperature conditions.

Fig. 12 is a performance curve under a variety of evaporation and condensation temperatures for the refrigerant mixture M1 at 60 Hz and 130 V.

Cylinder Pressure and Loss Analysis

The various characteristics of the compressor may be altered by using different refrigerants since changing the refrigerant results in changes in specific volume, adiabatic coefficient and other physical constants, it is thought that various characteristics of the compressor are also changed.

In order to understand these changes, the cylinder internal pressure and compressor losses were analyzed for each refrigerant for comparison.

The test compressor was a rolling piston, rotary type modified for experimental use.

For determination of compressor internal characteristics, and its refrigeration capacity is 3440 kcal/h and the cylinder volume is 22.32 cc/rev. and a constant speed of 50/60 Hz. The cylinder internal pressure was measured with piezoelectric transducer (Kisler). Crank angle signals were taken out with a LED and phototransistor couple. The refrigerant gas flow was measured with a "secondary refrigerant type compressor calorimeter."

The experimental conditions are shown in Table 5.

The various efficiency terms used are defiend below.

Table 5

Electric sources	100 V - 60/50 Hz
Evaporating temp.	0°C
Condensing temp.	50°C
Suction temp.	11°C

Table 6

Volume efficiency	$\eta_v = \frac{G_R}{V/v \cdot N}$
Motor efficiency	$\eta_{mo} = \frac{W_{out}}{W_{in}}$
Mechanics efficiency	$\eta_{me} = \frac{L_i}{W_{out}}$
Compression efficiency	$\eta_c = \frac{L_{th}}{L_i}$
Adiabatic efficiency	$\eta_{ad} = \frac{L_{th}}{W_{out}}$
Compressor efficiency	$\eta_{comp} = \frac{L_{th}}{W_{in}}$

G_R : flow rate
V : cylinder volume
v : specific volume of suction gas
N : revolution
W_{in} : input of motor
W_{out} : output of motor
L_i : power of diagram
L_{th} : power of theory

Figs. 13 and 14 are P-θ diagrams for R22 and refrigerant mixture M1 in the compression chamber. Figs. 15 and 16 are waveforms in the suction chamber.

I can be seen from these P-θ curves, that the pressure waveforms in the compresssion chamber are alike for the two refrigerants and there is no significant difference between the mono-component refrigerant and the binary refrigerant in the compression process. However, since the pressure peak values showed fair amounts of variations and the peak values are larger at higher frequencies and with larger flow rate, the discharged refrigerant per unit time seems to be a factor in inducing the above mentioned difference.

On the other hand, the pressure waveforms in the suction chamber are very much alike for both refrigerants. However, the pressure difference is slightly larger for refrigerant mixture M1. This is probably due to a difference in the suction refrigerant flow per unit time. Figs. 17 and 18 show the ratios of respective loses to total loss as calculated from the above-mentioned P-θ diagram.(2,3) For reference, the loss analysis for R12 is also shown. Since the motor input varies according to refrigerants, the respective loses are shown in percentage. The motor loss is the largest single loss element for both refrigerants.

Each of the losses are studied below.

(a) Heating loss during the suction and compression process

The second largest loss factor is heating loss during suction and compression process.

There is a large difference between refrigerants in this respect. Heating loss during the suction and compression process arises from the transfer of heat from the cylinder wall to the gas, oil leaks, etc., and appears to depend on the cylinder wall temperature, oil temperature, etc. The measured values of the discharge gas temperature, which are considered to be representative of cylinder wall temperature, oil temperature, etc., are shown in Table 7.

Table 7

Discharge temperature [°C]

Refrigerant	R22	R12	R13B1/R22
50 Hz	92.3	76.0	92.9
60 Hz	94.8	78.1	94.0

Compariosn of discharge temperature and heating loss shows that with R22 and refrigerant mixture M1 which have high discharge temperatures, the proportion of heating loss is also large, whereas with refrigerants having low discharge temperatures, such as R12, etc., heating loss accounts for only small proportions of total losses.

(b) Suction/discharge loss

Figs. 19 and 20 show the relation between suction, discharge loss and specific gravity of vapor.

From these results, it is apparent that the amount of loss is nearly proportional to the specific gravity of vapor and the rate of increase is higher with increasing frequency. The clearance volume loss is substantially unchanged for each refrigerant.

Suitability of Compressor Materials for Refrigerant

The compressor materials, including lubricating oil, component materials of the motor, etc., must also be selected to suit the refrigerant used.

(a) Solubility of refrigerants in oil

As the split type heat pump room air conditioner in this case is intended for use in cold districts, we need information on the critical resolution temperature (C.R.T.) of the lucricating oil-refrigerant.

Fig. 21 shows the C.R.T. of R13B1-lubricating oil in comparison with that of R22-lubricating oil. There is a fair difference in C.R.T. between the two refrigerants. We selected lubricating oil B having a low C.R.T.

(b) Lubrication characteristics at sliding pair

Modification of the refrigerant results in a change in the viscosity of refrigerant and lubricating oils. Moreover, the chemical properties of the refrigerant may influence the sliding characteristics.

A falex test was performed in order to evaluate the lubrication at the sliding pair of a mixture of refrigerant and lubricating oil.

The test was conducted under the conditions shown in Table 8 and the amount of wear, the coefficient of friction and the temperature of oil were measured.

Table 8 Falex test condition

Test No.	Load	Refrigerant	Wearing (mg) Pin	Blocks	Coefficient of friction 3 Hr	Temp. of oil ΔT(°C)
1	375 lbs	R22	0.2	0.5	0.095	49
2	"	R13B1/R22	0.4	0.4	0.105	50
3	"	R13B1	0.3	0.5	0.094	52

Based on the above results, it is understood that a change in refrigerant does not affect the sliding characteristics.

Table 9

Refrigerant	R13B1
Oil	B
Metal	Fe, Cu
Ratio	Ref./oil = 100 g/50 g

(c) Chemical properties of refrigerants

In order to understand the thermal stability of the R13B1 in the presence of metal and oil, a test was carried out using the sealed tube method. The conditions and results of the test are shown in Table 10. Fig. 22 is a graphic representation of the results.

It is apparent that the rate of degradation increases with increasing temperature. The long-term usable temperature presumed from the above results for R13B1 is slightly lower than that for R22.

Table 10

Refrigerant	Temperature (°C)	Time (days)	Acid of refrigerant (asHBr, ppm)
R13B1	150	14	1.5
R13B1	175	14	14
R13B1	200	14	0.30%
R13B1	150	30	6.0
R13B1	175	30	37
R13B1	200	30	0.95%

(d) Influence of the refrigerants mixture M1 on the electrical insulation system for the motor

Results of the sealed tube test and those of an accelerated live test in the actual compressor revealed that the insulating materials-polyester film, magnet wire sheath-amide-imide resin coating which are used in compressors using R22 today are suitable for use.

CONCLUSION

1. When the binary refrigerant R13B1/R22 (30/70) is used in a heat pump air conditioner, the heating capacity at low outdoor temperature is increased and, moreover, the EER is enhanced.
2. Since this refrigerant differs from R22, etc. in various characteristics, a compatible compressor design centered around compressor materials was attempted.
3. As a result, a air-source heat pump room air conditioner for cold districts has been successfully developed.

ACKNOWLEDGEMENT

The authors would like to express their thanks to Mr. Akira Nakazawa, Chief Engineer of Air-conditioner Division, and Mr. Yuji Yoshida, Chief Engineer of Corporate Engineering Division, Matsushita Electric Industrial Co., Ltd.

REFERENCES

1. Yoshida, Y. et al., "Thermodynamic Evaluation of Mixed Working Fluids", National Technical Report Vo. 29, No. 1 (Feb. 1983).
2. Wakabayashi, H. et al., "Analysis of Performance in a Rotary Compressor", Proc. Purdue Comp. Tech. Conf., 1982.
3. Hirano, H., "Analysis of Suction Passage loss in a Rotary Compressor", Proc. Purdue Comp. Tech. Conf., 1984.

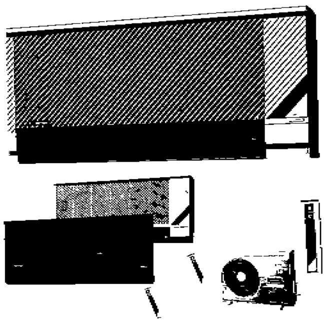

Fig 1

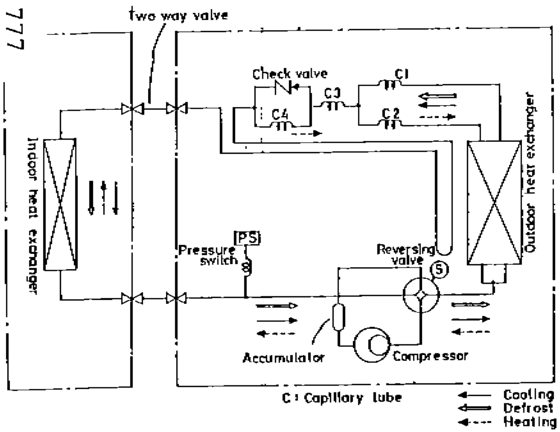

Fig 2

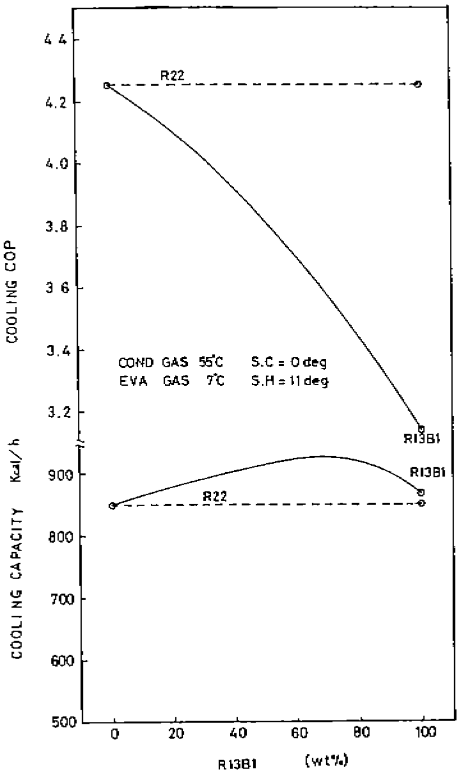

Fig 3

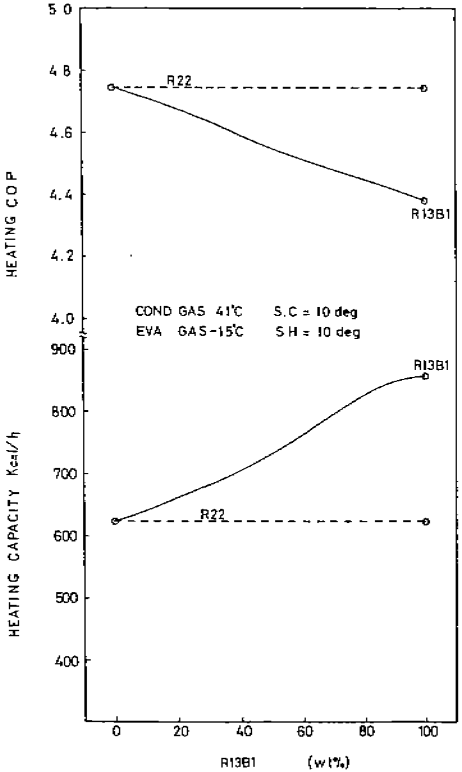

Fig 4

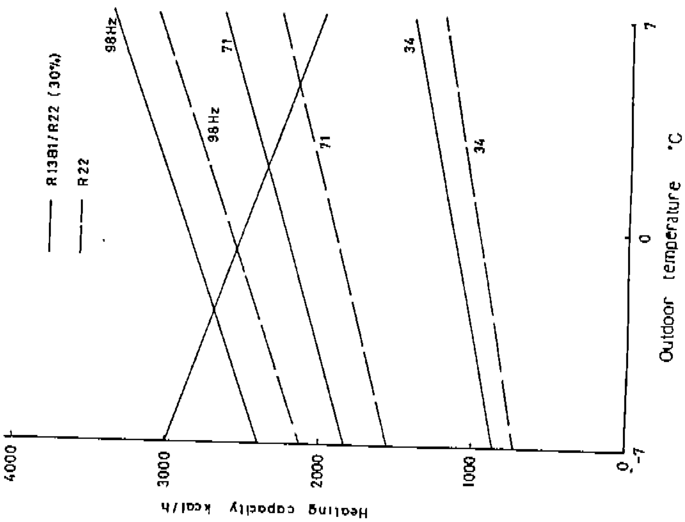

R13B1/R22 (30%)
R22
98Hz
71
34
Heating capacity kcal/h
4000
3000
2000
1000
0
-7
0
7
Outdoor temperature °C

Fig 6

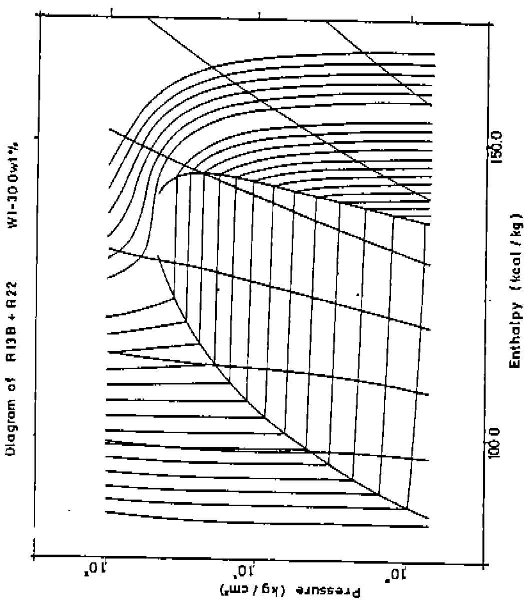

Diagram of R13B + R22 Wt-30.0wt%
Pressure (kg/cm²)
Enthalpy (kcal/kg)
100.0
150.0

Fig 5

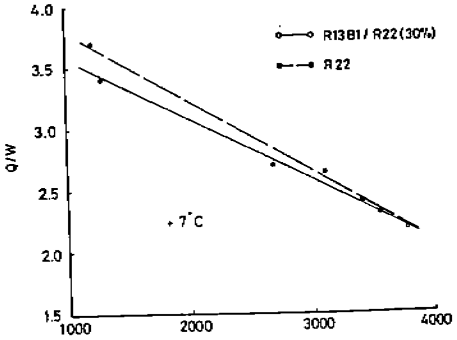

Fig 7

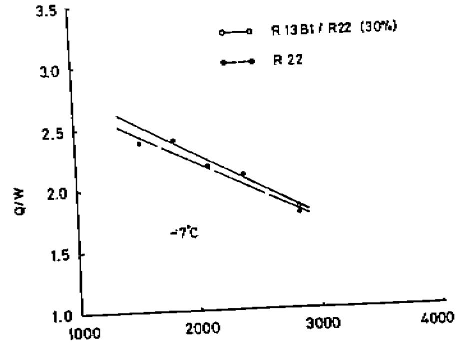

Fig 8

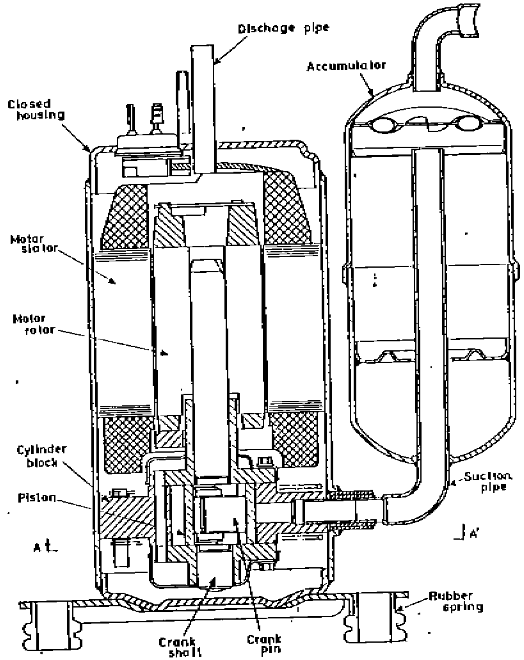

Fig 9 a

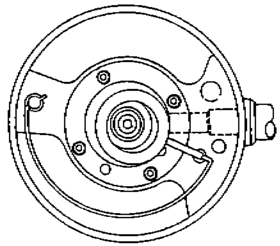

Fig 9 b

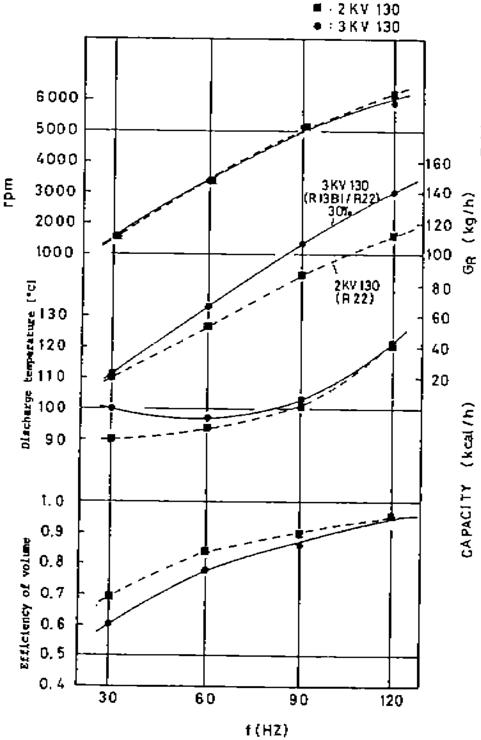

Fig 10.

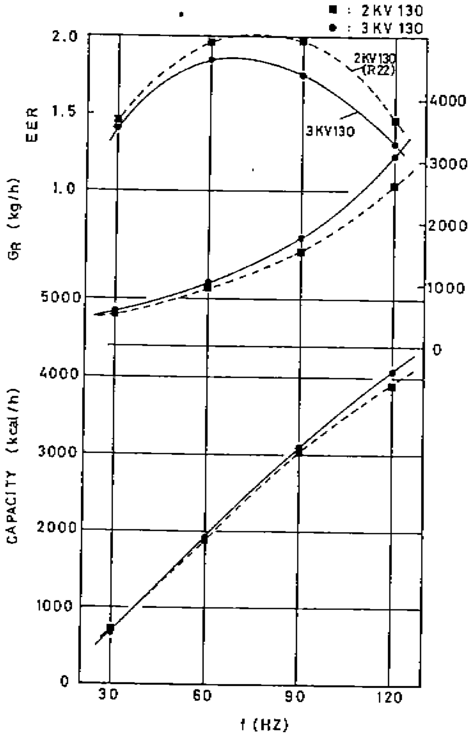

Fig 11

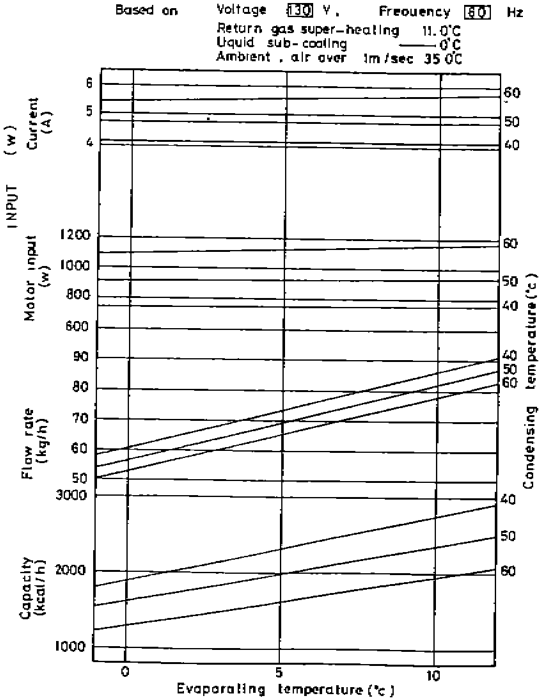

Fig 12

780

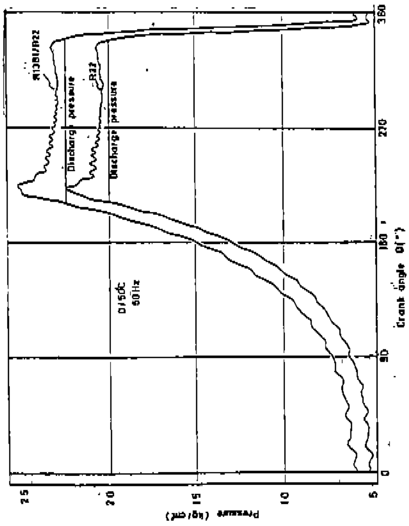

Fig 13

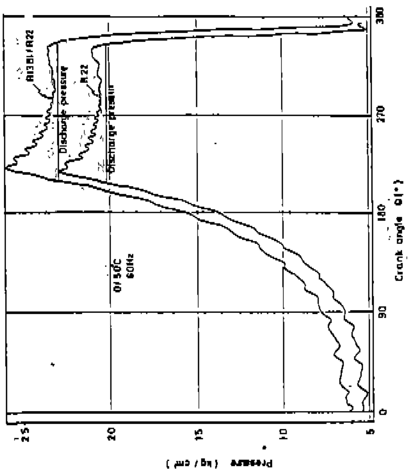

Fig 14

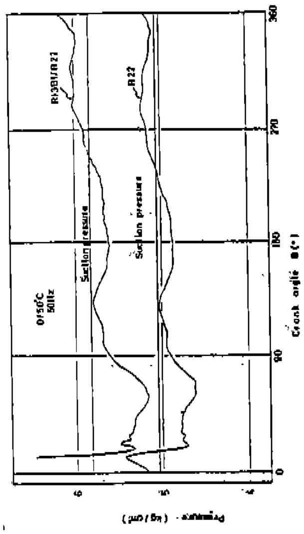

Fig 15

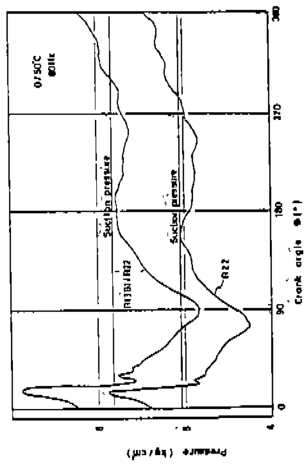

Fig 16

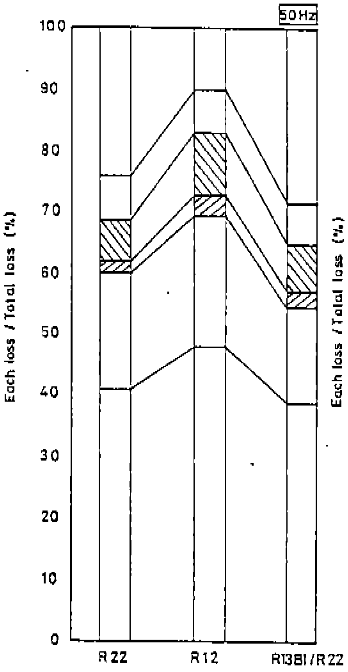

Fig 17

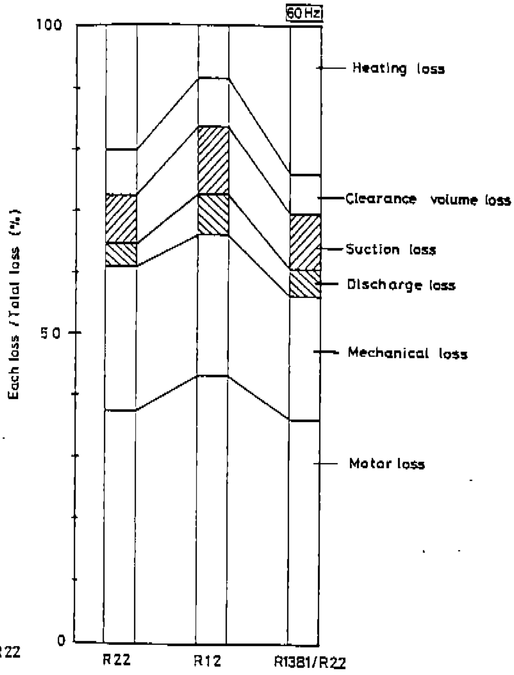

Fig 18

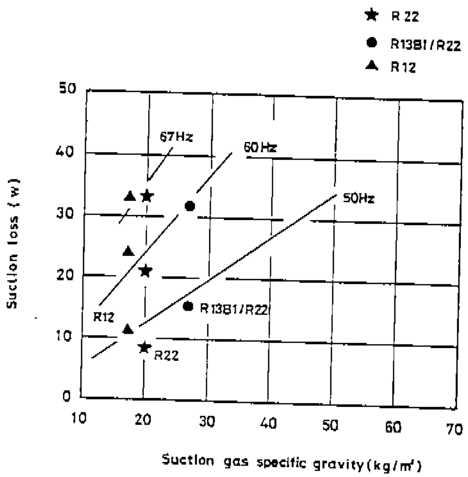

Fig 19

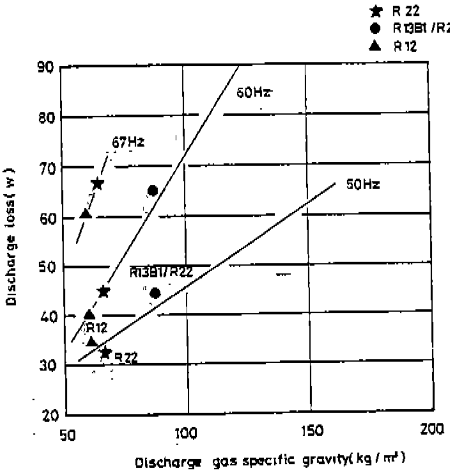

Fig 20

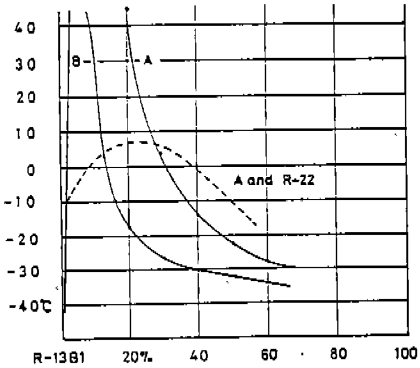

Fig 21

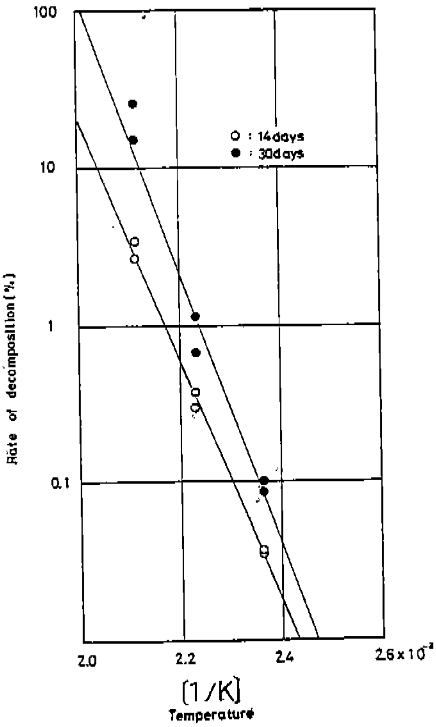

Fig 22